The role of nutricline depth in regulating the ocean carbon cycle

Pedro Cermeño[a], Stephanie Dutkiewicz[b], Roger P. Harris[c], Mick Follows[b], Oscar Schofield[a], and Paul G. Falkowski[a,d,1]

[a]Environmental Biophysics and Molecular Ecology Program, Institute of Marine and Coastal Sciences, Rutgers University, 71 Dudley Road, New Brunswick, New Jersey, 08901; [b]Department of Earth, Atmospheric, and Planetary Sciences, 77 Massachusetts Avenue, Massachusetts Institute of Technology, Cambridge, MA 02139-4307; [c]Plymouth Marine Laboratory, Prospect Place, Plymouth PL1 3DH, United Kingdom; and [d]Department of Earth and Planetary Science, Rutgers University, 610 Taylor Road, Piscataway, New Jersey 08854

Carbon uptake by marine phytoplankton, and its export as organic matter to the ocean interior (i.e., the "biological pump"), lowers the partial pressure of carbon dioxide (pCO_2) in the upper ocean and facilitates the diffusive drawdown of atmospheric CO_2. Conversely, precipitation of calcium carbonate by marine planktonic calcifiers such as coccolithophorids increases pCO_2 and promotes its outgassing (i.e., the "alkalinity pump"). Over the past ≈100 million years, these two carbon fluxes have been modulated by the relative abundance of diatoms and coccolithophores, resulting in biological feedback on atmospheric CO_2 and Earth's climate; yet, the processes determining the relative distribution of these two phytoplankton taxa remain poorly understood. We analyzed phytoplankton community composition in the Atlantic Ocean and show that the distribution of diatoms and coccolithophorids is correlated with the nutricline depth, a proxy of nutrient supply to the upper mixed layer of the ocean. Using this analysis in conjunction with a coupled atmosphere–ocean intermediate complexity model, we predict a dramatic reduction in the nutrient supply to the euphotic layer in the coming century as a result of increased thermal stratification. Our findings indicate that, by altering phytoplankton community composition, this causal relationship may lead to a decreased efficiency of the biological pump in sequestering atmospheric CO_2, implying a positive feedback in the climate system. These results provide a mechanistic basis for understanding the connection between upper ocean dynamics, the calcium carbonate-to-organic C production ratio and atmospheric pCO_2 variations on time scales ranging from seasonal cycles to geological transitions.

coccolithophorids | diatoms | stratification | climate change

Phytoplankton have evolved over hundreds of millions of years, interacting with physics, chemistry, and neighboring organisms to produce a great diversity of morphological groups and life forms. This polyphyletic group of aquatic organisms includes nearly 25,000 morphologically defined species distributed among eight major divisions or phyla (1). In the ocean, these organisms are central to biogeochemical and ecological services, linking metabolic sequences and properties to form a continuous network of elemental fluxes. Among this diverse group of photosynthetic organisms, diatoms and coccolithophorids in particular play key roles in the regulation of atmospheric pCO_2 and the maintenance of upper trophic levels (1–7).

Although diatoms and coccolithophorids are derived from a common Rhodophyte ancestor, evolutionary divergence and selection led these two phytoplankton functional groups to distinct ecological superniches that have significant biogeochemical implications (1). In the modern ocean, diatoms dominate the export flux of carbon, contributing significantly to the long-term sequestration of atmospheric CO_2 in the ocean interior (6). Coccolithophorids, in contrast, through the formation of calcium carbonate ($CaCO_3$) shells, alter the inorganic carbon system and alkalinity of seawater and release CO_2, which may escape to the atmosphere (2, 3). Hence, the balance between diatoms and coccolithophorids potentially influences the $CaCO_3$

to organic carbon export ratio, a major factor determining the partitioning of CO_2 between the atmosphere and ocean.

From an evolutionary perspective, diatoms and coccolithophorids constitute an example of the classical ecological divergence of *r*- and *K*-strategists (8). Diatoms, as opportunists (*r*-strategists), efficiently exploit resources in unstable, rarefied environments (8, 9). In contrast, coccolithophorids, possessing a high affinity for nutrients and low resource requirements (*K*-strategists), generally grow under quiescent conditions characteristic of stratified, open ocean waters (7). Based on their physiological features and response to resource supply dynamics, the ecological distribution of these two phytoplankton taxa has been hypothesized to be linked to the mechanisms that supply nutrients to the upper mixed layer of the ocean (8, 10). Here, we analyze observations of phytoplankton biomass and species composition along with concurrent measurements of hydrographic variables from four Atlantic Meridional Transects (AMTs) (Fig. 1*A*) to elucidate processes controlling the balance between diatoms and coccolithophorids in the ocean and their role in the carbon cycle. We then apply our diagnostic analyses to a coupled atmosphere–ocean intermediate complexity model to make projections about the potential response of these two phytoplankton taxa in the coming century.

Results and Discussion

Diatoms and Coccolithophorids in the Atlantic Ocean. Across latitudinal gradients in the ocean, the availability of inorganic nutrients exerts a major control on phytoplankton biomass, primary productivity, and community structure (11). Typically, high latitude, temperate, and upwelling systems receive substantial amounts of nutrients from deep waters via wind-driven vertical mixing and transport along isopycnal layers. In contrast, phytoplankton communities inhabiting low latitude environments, such as stratified, subtropical gyres, largely rely on local recycling and diapycnal nutrient fluxes to sustain their standing stocks. Our data analysis suggests that the biomass (and biovolume) of both diatoms and coccolithophorids increases consistently from subtropical regions to temperate and upwelling systems in response to increased nutrient supply (Fig. 1*B*). Although both phytoplankton groups exhibited similar latitudinal trends in biomass, our results reveal striking differences in their ranges of variation. Diatom biomass increased more than five orders of magnitude from low latitudes to temperate and upwelling systems, whereas coccolithophorid standing stocks varied by only two orders of magnitude (Fig. 1*B*). The variations in diatom and coccolithophorid biomass are further reflected in their patterns
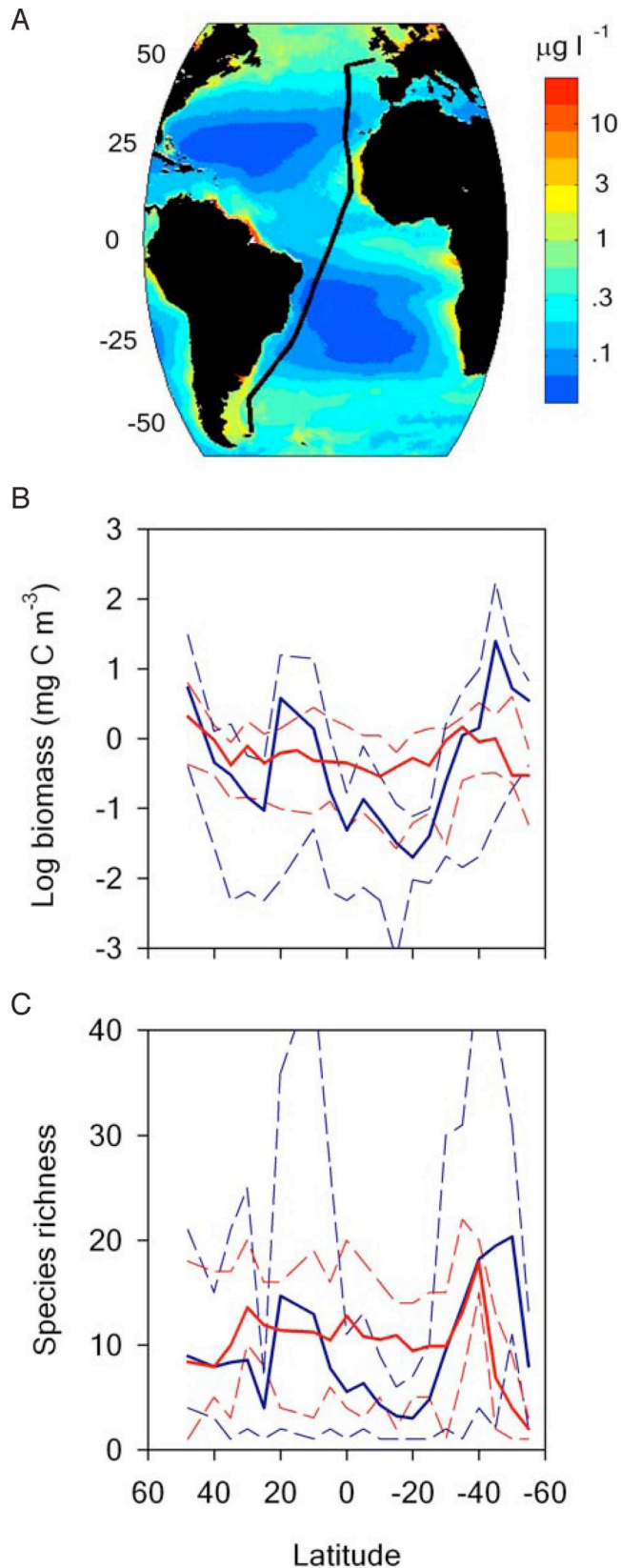
A

B

C

Fig. 1. Phytoplankton distribution in the Atlantic Ocean. (*A*) AMT cruise tracks overlain on an annual climatology of chlorophyll showing high values where surface nutrients are elevated. (*B*) Latitudinal distribution of biomass of diatoms (blue) and coccolithophorids (red). (*C*), as in *B*, but for number of species. Solid lines in panels b and c are biomass and number of species averaged each 5° of latitude. Dashed lines are the range of data values.
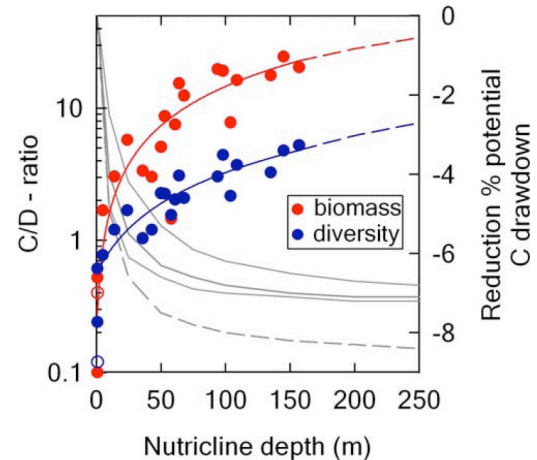
Fig. 2. Nutricline depth controls the coccolithophorid-to-diatom (C/D) ratio. Data points are 5° zonal averages of C/D ratio and nutricline depth from four Atlantic latitudinal transects (solid circles) and a coastal station in the English Channel (open circles). The left *y* axis is represented on a log scale to highlight the rapid shift from diatoms to coccolithophorids in response to the onset of water column stratification and nutrient depletion. Color lines denote the least square linear regression models: y(biomass) $= 0.14 + 0.14\,x$; $R^2 = 0.78$; $P < 0.0001$, and y(diversity) $= 0.55 + 0.03\,x$; $R^2 = 0.83$; $P < 0.0001$. Changes (%) in the biological potential for C drawdown were estimated from the model equation (C/D ratio vs. nutricline depth) considering the opposing effects of photosynthesis and calcification (thick solid gray line, see Methods for details), and the 95% confidence intervals (thin gray lines). Note that the transition from diatoms to coccolithophorids is linked to the stabilization/destabilization of water column. Reduction in pump's efficiency considering changes in the buffering capacity of the ocean's carbonate system in a future, high CO_2 scenario was also displayed (dashed gray line).

of diversity. The number of diatom species increased rapidly from subtropical to temperate and upwelling systems; morphologically distinct diatom species were twofold greater than that of coccolithophorids (Fig. 1*C*).

There is a striking correspondence between the coccolithophorid-to-diatom (C/D) ratio and depth of the nutricline (Fig. 2). Specifically, our analysis indicates that, across the entire geographic range considered, coccolithophorids rapidly rise to dominance relative to diatoms as the water column stratifies and the nutricline deepens.

The depth of the nutricline depends on the degree of water column stratification and the magnitude of momentum transfer associated with wind stress (12). When physical mixing increases, the upper mixed layer penetrates the nutricline, thereby providing a source of nutrients to the euphotic zone; nutrients become elevated throughout the upper water column (i.e., zero-depth nutricline in this study). Conversely, when thermal stratification increases, the upper water column is deprived of nutrients, leading to a progressive deepening of the nutricline that closely parallels the depth of the euphotic layer. In open ocean subtropical systems, the upper water column shows a marked temperature gradient all of the way to the surface and, to large extent, nutrient entrainment is limited to diffusive processes. Hence, to first order, the depth of the nutricline reflects nutrient supply into the upper mixed layer. In fact, across the latitudinal gradient considered in this study, the primary productivity of phytoplankton is negatively correlated with the depth of the nutricline (data not shown). This inverse relationship suggests a strong coupling between the position of the nutricline in the water column, the rate of nutrient supply into the euphotic layer and the photosynthetic performance of phytoplankton (13).

Different factors, such as the availability of orthosilicic acid (14), the mineral used by diatoms to construct their cell walls, or

the saturation state of seawater with respect to calcium carbonate, a key controller of calcification (15), have been put forward to explain the distribution of diatoms and coccolithophorids in different marine environments. For instance, the low silicate-to-nitrate input ratios characteristic of the equatorial Pacific Ocean have been suggested to limit diatom productivity and C drawdown in that high nutrient-low biomass ocean region (14). It is conceivable that the positive relationship reported here between the nutricline depth and the C/D-ratio could be driven by differences in the silicate-to-nitrate input ratio at the base of the thermocline. However, assuming that coccolithophorids are more efficient than diatoms in nutrient acquisition at low concentrations (7–9), an increase in the silicate-to-nitrate input ratio would decrease the C/D-ratio only in the following scenarios: (a) if upper ocean turbulence (or nutrient supply) also increases, which is consistent with our relationship between the C/D-ratio and the nutricline depth; or (b) in high nutrient, low chlorophyll regions such as the Equatorial Pacific where both silicate and iron are thought to co-limit diatom productivity (16). Therefore, although these factors may play a role, our study, covering temperate, upwelling, tropical, subtropical, and equatorial ecosystems, supports the hypothesis that upper ocean turbulence and nutrient supply dynamics exert a dominant control on the ecological selection and evolutionary success of these two phytoplankton functional groups. Moreover, a suite of competition experiments in continuous culture systems supports the model predictions (10) that the population dynamics of diatoms and coccolithophorids can be controlled simply by varying the rate of nitrate supply; the C/D-ratio varies in response to the rate of nutrient pulses (unpublished results). Remarkably, the strong linkage between the nutricline depth and phytoplankton community composition reported here arises despite that, in nature, ecological systems are influenced by manifold and ever changing environmental templates and complex biotic interactions.

Our field observations clearly illustrate how the balance between diatoms and coccolithophorids primarily is driven by variations in diatom biomass and diversity, with coccolithophorids exhibiting comparatively minor response to environmental variability (Figs. 1B, 1C). Why, however, do these phytoplankton groups exhibit such different ranges of variability?

The global biogeography of phytoplankton is determined by local environmental factors that select for a particular species based on its optimal growth potential. According to this "universal distribution, local selection rule" (7), the patterns depicted here for diatoms and coccolithophorids reflect their divergent life histories and survival strategies (8). Diatoms, by virtue of high maximum growth rates, luxury nutrient uptake, and the ability to store inorganic nutrients in vacuoles, exploit unstable environments where resources are supplied in excess relative to biological demand. Often, these organisms form massive blooms (6). However, adaptation to unstable environments imposes severe nutritional constraints under stable conditions. Prolonged stability, such as increased ocean stratification, drives planktonic ecosystems to operate near their carrying capacity (i.e., resource demand-to-supply ratio close to unity); and, under these conditions, ecological selection depends primarily on the ability of an individual species to compete for limited resources (17). With the exception of species that migrate vertically and take up inorganic nutrients in the vicinity of the nutricline, or that have formed symbiotic associations with nitrogen fixers, diatoms are at a disadvantage under strong resource limitation because of their high nutritional requirements and high half-saturation constants. Consequently, across contrasting marine environments, the distribution of diatoms is inextricably tied to ample variations in biomass and diversity (Fig. 1B, 1C). In contrast, coccolithophorids have lower maximum nutrient uptake and growth rates (7, 18). Instead, they possess low half-saturation constants for nutrient uptake and small intracellular nutrient

quotas (i.e., low nutritional requirements) (9). These ecophysiological features allow coccolithophorids to inhabit a broad array of open ocean environments without succumbing to dramatic variations in standing stocks (Figs. 1B, 1C). It is noteworthy that satellite image analyses, based on the light scattering by coccoliths, have highlighted massive blooms of coccolithophorids at high latitudes in the world oceans (7). Although these blooms may have a significant impact on regional scales, they represent a minor fraction compared with the background levels of calcium carbonate produced on an annual basis and a global spatial scale (19).

The impact of nutrient limitation on the competitive success of diatoms and coccolithophorids has profound implications. Changes in the C/D-ratio may alter the efficiency of the biological pump by controlling the balance between two key processes: (a) export of carbon into the ocean interior, and (b) release of CO_2 because of coccolithophorid calcification (each mole $CaCO_3$ precipitated results in ≈ 0.7 mole CO_2 released, assuming present CO_2 concentrations, temperature of 12 °C and salinity of 35) (3). Consequently, for a given rate of organic productivity, an increase in the C/D ratio will lead to a decreased role of the biological pump in sequestering atmospheric CO_2 (3, 20). Our analysis suggests that major changes in the C/D ratio are linked to the stabilization-destabilization of the water column (Fig. 2). Low latitude, stratified ecosystems are dominated by coccolithophorids (i.e., C/D ratio $\gg 1$), and therefore increased thermal stratification has little effect on the particulate inorganic carbon to particulate organic carbon production ratio. However, in unstable environments, characterized by a significant contribution of diatoms, the onset of water column stratification and subsequent nutrient depletion cause a rapid increase in the C/D ratio and reduce, to a far greater extent, the efficiency of the biological pump (Fig. 2). This rapid change from diatom to coccolithophorid-dominated assemblages in response to nutrient supply dynamics provides a mechanistic basis for understanding variations in the $CaCO_3$ to organic C production ratio.

Future Projections in a Warmer Ocean. Current evidence and modeling analyses suggest that climate warming will increase ocean stratification, and hence reduce nutrient exchange between the ocean interior and the upper mixed layer (21, 22). Indeed, climate-driven trends in upper ocean stratification and primary productivity across the central, oligotrophic gyres are already detectable and may be occurring faster than model predictions (23, 24). Yet, predicting the impact that these changes may exert on the ecological functioning of marine ecosystems remains elusive. To investigate possible changes in the distribution of diatoms and coccolithophorids caused by climate warming, we projected our data-driven model of the relationship between the C/D-ratio and the nutricline depth onto a coupled atmosphere-ocean intermediate complexity model (GCM) (see Methods for details). Our three dimensional model was forced by the Intergovernmental Panel on Climate Change (IPCC) IS92a "continually increasing" CO_2 scenario (956 p.p.m.v. in the year 2100). By the end of this century, in this model configuration and CO_2 scenario, the increased upper ocean stratification reduces the supply of macronutrients to the euphotic layer, deepens the nutricline and leads to a reduction in global oceanic primary productivity of 14% (25). Assuming that the relationship between C/D-ratio and nutricline depth is robust on time scales of centuries, the coupled intermediate complexity model further predicts a dramatic increase in the C/D ratio across vast areas in the North Atlantic, but the effect is particularly pronounced in temperate ecosystems (Fig. 3). By the year 2100, the C/D ratio in the North Atlantic temperate region is projected to increase by >80% relative to year 2000. In both hemispheres, the expansion of subtropical systems into temperate, equatorial and upwelling regions causes striking shifts in ecosystems character-
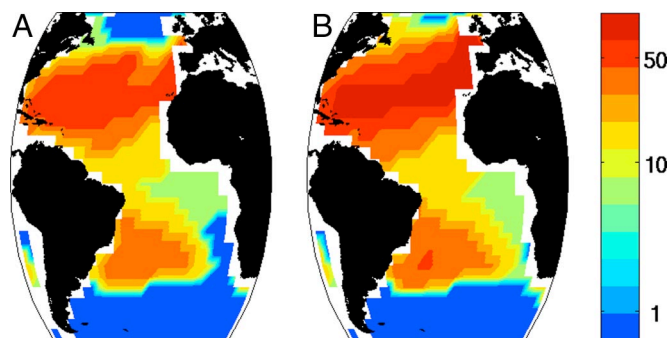
Fig. 3. Modeled change in the distribution of diatoms and coccolithophorids projected in the coming century. (*A*) Coccolithophorid-to-diatom (C/D) biomass ratio in year 2000. (*B*), as in *A*, but for 2100 (assuming IPCC IS92 CO_2 ''continually increasing'' scenario).

Fig. 4. Sensitivity of the biogeochemical control associated with shifting the coccolithophorid-to-diatom (C/D) ratio to variations in coccolithophorid calcification and the C/N stoichiometry. Changes (%) in the efficiency of the biological pump by the end of this century were calculated from the opposing effects of photosynthesis and calcification according to our projections of the C/D-ratio (1-lambda as a percentage between 2000 and 2100; see Materials and Methods for details). (*A*) is for the whole Atlantic Ocean and (*B*) is for the North Atlantic temperate province. Solid black line represents zero change in efficiency of the biological pump. We assumed an initial carbon-to-nitrogen (C/N) ratio of 6.6. Number positions represent approximately the constraint limits to changes in C/N ratio and coccolithophorid calcification according to experimental studies simulating the response of phytoplankton C physiology to elevated pCO$_2$. Letters refer to references used (a, 29 and 42; b, 30; c, 31; d, 43; e, 44; f, 45 for *Skeletonema costatum*). When the C/N ratio or the change in coccolithophorid calcification were not specified, we assumed Redfield ratio (6.6) and no change in calcification.
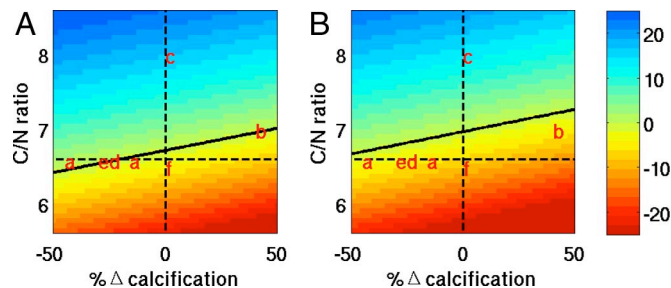
ized in the present day by a significant contribution of diatoms (Fig. 3).

Our analysis yields quantitative predictions of the relative response of diatoms and coccolithophorids to climate warming (i.e., not absolute changes in their standing stocks). Based on experimental work (7, 9), field observations (Figs. 1*B*, 1*C*), and modeling analyses (26, 27), we suggest that enhanced nutrient limitation will reduce the competitive advantages of diatoms. In contrast, this particular scenario is expected to be less detrimental for other phytoplankton groups such as coccolithophorids or picophytoplankton (20, 28). Their low nutritional requirements could play a decisive role if, as expected, mineral nutrient limitation increases in a warmer ocean.

Our prognostic model results indicate that in a climate warming scenario, the progressive stratification of oceanic systems will increase the C/D ratio, reducing the potential of marine plankton ecosystems to drawdown atmospheric CO_2 (20). The model further predicts that oceanic regions subjected to the influence of the expansive subtropical gyres, such as the North Atlantic drift province or tropical upwelling systems, could be particularly susceptible to this biogeochemical control (Fig. 3). The sensitivity of these oceanic regions to this biological feedback is associated with two factors. First, ocean general circulation models find the North Atlantic region as an area particularly susceptible to climate warming. Second, these ocean regions are characterized by a significant contribution of diatoms to total phytoplankton biomass, and therefore a slight stratification would cause dramatic changes in the C/D ratio.

Changes in the carbonate system of seawater may also contribute with a positive feedback by altering the released CO_2 to precipitated $CaCO_3$ ratio or "Revelle factor" (ψ). This ratio increases with increasing seawater pCO$_2$, and decreasing temperature and salinity (3). The projections of atmospheric pCO$_2$ by the end of this century, and its invasion into ocean systems will double or triple seawater pCO$_2$ in the surface ocean. Doubling the current pCO$_2$, and warming the water by 8 °C, will increase ψ to 0.79 rather than 0.69 estimated for present day conditions. Therefore, a substantial part of the projected reduction in the efficiency of marine ecosystems to drawdown atmospheric CO_2 would be caused by parallel changes in the buffering capacity of the ocean's carbonate system.

The efficiency of the biological pump could also change if the invasion of anthropogenic CO_2 into the ocean alters the rates of coccolithophorid calcification (29, 30) and/or phytoplankton C consumption (hence leading to a deviation in the C/N ratio from 106:16) (31). Currently, there is enormous uncertainty about the response of phytoplankton physiology to elevated seawater pCO$_2$. For instance, experimental analyses, simulating high CO_2 concentrations, indicate that the rate of coccolithophorid calci-

fication can decrease, increase or be species-specific. We conducted a sensitivity analysis to investigate the significance of these changes on the biogeochemical control described in this study (i.e., increased C/D-ratio) (Fig. 4). First, the biogeochemical control described here (positive feedback on atmospheric pCO$_2$) could be of a magnitude comparable, but inverse to, experimentally observed reductions in coccolithophorid calcification. Second, if calcification increases (30), the storage capacity of the surface ocean for CO_2 would decrease, which, when added to the reduced ability of marine ecosystems to drawdown atmospheric CO_2 reported here, would cause an even larger decline in the efficiency of the biological pump (Fig. 4). Third, an increase in the C/N ratio of phytoplankton (and export production) (31), would offset the biogeochemical controls associated with both an increase in C/D-ratio and coccolithophorid calcification, increasing the ability of marine ecosystems to absorb atmospheric CO_2. Our analysis of data from the literature suggests a slight positive feedback (i.e., most of references lie below the black solid line in Fig. 4). However, these results must be considered cautiously, as it remains uncertain to what extent experimental simulations, based on short-term analyses (weeks) and a limited spatial scale, may be representative of the long-term functioning of marine pelagic ecosystems in nature.

Concluding Remarks. Over the past ≈100 million years, diatoms and coccolithophorids have responded to climatically forced changes in upper ocean turbulence and nutrient exchange dynamics, leading to a feedback in the regulation of atmospheric pCO$_2$ and Earth's climate (5, 7, 32). Consistent with the geological record and the classical "Mandala" of Margalef (8), our results indicate that the relative distribution of diatoms and coccolithophorids is strongly dependent upon the mechanisms that supply nutrients into the upper mixed layer of the ocean. We suggest that this mechanistic connection is the major factor responsible for the succession and regime shifts of these two phytoplankton functional groups in the ocean. If so, these taxonomic shifts, and their associated impact on net air–sea CO_2 exchange, would be linked mechanistically to the seasonal dynamics of the upper mixed layer, interannual variations in

ECOLOGY

climatic forcing (33), contemporaneous trends in anthropogenic climate warming (20, 27), and historical climate change (32, 34).

Materials and Methods

Sampling. Physical, chemical, and biological variables were obtained from four Atlantic Meridional Transect cruises: September–October 1995, April–May 1996, September–October 1996, and April–May 1997. Micromolar concentrations of inorganic nutrients were determined on fresh samples using a Technicon AAII AutoAnalyser and standard techniques. For each station, the depth of the nutricline was taken to be the first depth where nitrate was detected (> 0.05 μmol/l).

Microscopic Analysis. A total of 224 samples were collected for the identification and counting of nano- and microplankton at the surface, the bottom of the euphotic layer and, in some cases an intermediate depth. Duplicate 100-ml samples were preserved in 1% Lugol's iodine solution and 0.5% buffered formalin. Samples were allowed to settle in sedimentation chambers for 2–3 days. Cells were counted, measured, and identified under an inverted microscope. Cell volume was calculated by assigning different geometric shapes that were most similar to the real shape of each phytoplankton species. Cell numbers were converted into carbon (C) biomass using biovolume estimates and conversion factors (35).

Determination of Primary Productivity. Primary productivity rates were determined using the ^{14}C-uptake technique after simulated *in situ* incubations (from dawn to dusk). After incubation, the samples were filtered at low-vacuum pressure (<100 mm Hg), through glass-fiber filters or polycarbonate filters (0.2 μm nominal pore size). Filters were exposed to concentrated HCl fumes overnight to remove the inorganic ^{14}C not incorporated biologically into the cells. The filters were then transferred to scintillation vials to which 4 ml of scintillation mixture was added. Radioactivity on each sample was determined on a Beckman LS6000 SC scintillation counter. Dark-bottle ^{14}C-activity was subtracted from the activity obtained in the light samples.

Numeric Simulation of Change in Ocean Nutrient Distribution and Export Production Over the 21th Century. The numeric simulation of change in ocean nutrient distribution was performed using the MIT-Integrated Global System Model (IGSM) 2.3, an earth system model of intermediate complexity (25). The atmospheric component is a zonally averaged primitive equation model (36) adapted from the GISS GCM Model II (37). There are 11 vertical levels and a latitudinal resolution of 4°. Each zonal band may consist of land, land-ice, ocean, and sea-ice. Surface temperature, turbulent and radiative fluxes and their derivatives are calculated over each type of surface. The terrestrial model is comprised of the Community Land Model for surface-heat fluxes and hydrological processes, the Terrestrial Ecosystems Model for the carbon dynamics of terrestrial ecosystems; and Natural Emissions Model, for the methane and nitrogen exchange.

The ocean component is the MIT general circulation model (38, 39) configured with 4° horizontal resolution, 15 vertical layers and realistic bathymetry. The Gent and McWilliams (40) mixing scheme is implemented to parameterize the effect of mesoscale eddies. Embedded in the ocean model is a thermodynamic sea-ice model. There is an explicit C cycle model with a parameterization of the biological export production limited by the availability of light and nutrients. This biogeochemical component follows the fate of a macronutrient, dissolved organic matter, alkalinity, and dissolved inorganic carbon. The current ocean macronutrient distribution compares very well with observations. A fixed export-ratio (export to total production ratio) and rain-ratio (calcium carbonate to organic carbon ratio) are assumed in this model. The nutricline depth is derived from the model as the depth where nitrate concentration first becomes more than 0.05 μmol/l NO_3.

The system is spun up for 2000 years to a statistical steady state with greenhouse gas concentrations of year 1860. The simulation is then run from 1860 to 1990 with observed greenhouse gas concentrations. From 1990 to 2100, the Emissions Prediction and Policy Analysis (41) model is used to predict greenhouse gas emissions from nations around the world through estimations of population and economic growth. In the scenario presented here, there is an assumption of no policy implementation to curb emissions, in a ''business-as-usual'' case.

By 2100, in this model configuration, the atmospheric pCO$_2$ concentration reaches 956 p.p.m.v., which, on average, raises surface air temperature by 4 °C and the sea surface temperature by 2.7 °C. The increased stratification in the surface waters reduces the supply of macronutrient to the euphotic layer, deepens the nutricline, and decreases biological productivity (25). On an annual basis, the oligotrophic conditions of the subtropical gyres become more pronounced and expand into temperate and equatorial latitudes.

Carbon Drawdown and Sensitivity to Changes in Phytoplankton C Physiology Induced by Elevated pCO$_2$. The potential of marine phytoplankton assemblages to drawdown atmospheric CO$_2$ was calculated from the opposing effects of photosynthesis and calcification. We defined λ as the C released as CO$_2$ due to coccolithophorid calcification divided by the total organic C mass of diatoms and coccolithophorids. Note that λ represents the grams of C released per gram of C biomass produced. Consequently, 1-λ can be assumed to represent the effective carbon flux that contributes to the absorption of atmospheric CO$_2$ (i.e., in the text referred to as the biological potential for atmospheric CO$_2$ drawdown or efficiency of the biological pump).

We calculated 1-λ for the years 2000 and 2100 according to the following equations:

$$1 - \lambda_{2000} = 1 - \frac{\theta \cdot \alpha \cdot \beta \cdot \psi_1}{\theta + 1}$$

$$1 - \lambda_{2100} = (1 \times \chi) - \frac{\theta \cdot \alpha \cdot \beta \cdot \psi_2 \cdot \delta}{\theta + 1}$$

where θ is the coccolithophorid to diatom biomass ratio that represents the organic C biomass of coccolithophorids relative to that of diatoms set as 1, α is the CaCO$_3$-to-organic C production ratio of coccolithophorids (here considered as 1:1), β is the CaCO$_3$ to C molecular weight (which converts grams of CaCO$_3$ into moles of CaCO$_3$ and then, after multiplying by the ''Revelle factor,'' yields the grams of C released as CO$_2$), ψ_1 or Revelle factor accounts for the moles of CO$_2$ released by mole of CaCO$_3$ precipitated, which is modulated by the buffering capacity of the ocean's carbonate system (3), and ψ_2 is as ψ_1 but by 2100 assuming Intergovernmental Panel on Climate Change predictions of CO$_2$ rise (IS92a ''continually increasing'' CO$_2$ scenario, 956 p.p.m.v. in the year 2100). Changes in θ between 2000 and 2100 were calculated by projecting our data-driven model of the relationship between the C/D ratio and the nutricline depth onto a coupled atmosphere–ocean intermediate complexity model (described above). δ and χ are calcification and C-uptake factors, respectively, used to estimate the sensitivity of the biogeochemical control associated with shifting the C/D ratio to changes in phytoplankton C physiology (e.g., calcification and/or C-overconsumption). We gave δ the values from 0.5 (-50%) to 1.5 (50%), and χ took the range from 0.85 to 1.3 (i.e., assuming we are presently in Redfield, these values would alter Redfield ratio from 5.6 to 8.6). Our results were compared with previous studies simulating the response of phytoplankton C physiology to increased seawater pCO$_2$ (29–31, 42–45)

1. Falkowski PG, *et al.* (2004) The evolution of modern eukaryotic phytoplankton. *Science* 305:354–360.
2. Volk T, Hoffert MI (1985) in *The Carbon Cycle and Atmospheric CO₂: Natural Variations Archean to Present*, eds Sundquist ET, Broecker WS (American Geophysical Union, Washington, DC) pp 99–110.
3. Frankignoulle M, Canon C, Gattuso J-P (1994) Marine calcification as a source of carbon dioxide: Positive feedback of increasing atmospheric CO₂. *Limnol Oceanog* 39:458–462.
4. Holligan PM, Robertson JE (1996) Significance of ocean carbonate budgets for the global carbon cycle. *Glob Change Biol* 2:85–95.
5. Falkowski PG, Barber RT, Smetacek V (1998) Biogeochemical controls and feedbacks on marine primary productivity. *Science* 281:200–206.
6. Smetacek V (1999) Diatoms and the ocean carbon cycle. *Protist* 150:25–32.
7. Iglesias-Rodríguez MD, *et al.* (2002) Representing key phytoplankton functional groups in ocean carbon cycle models: Coccolithophorids. *Glob Biogeochem Cycles* 16, 1100, doi: 10.1029/2001GB001454.
8. Margalef R (1978) Life forms of phytoplankton as survival alternatives in an unstable environment. *Oceanol Acta* 1:493–509.
9. Litchman E, Klausmeier CA, Schofield O, Falkowski PG (2007) The role of functional traits and trade-offs in structuring phytoplankton communities: Scaling from cellular to ecosystem level. *Ecol Lett* 10:1170–1181.
10. Tozzi S, Schofield O, Falkowski PG (2004) Historical climate change and ocean turbulence as selective agents for two key phytoplankton functional groups. *Mar Ecol Prog Ser* 274:123–132.

11. Longhurst AR, Sathyendranath S, Platt T, Caverhill C (1995) An estimate of global primary production in the ocean from satellite radiometer data. *J Plank Res* 17:1245–1271.
12. Denman KL, Gargett AE (1983) Time and space scales of vertical mixing and advection of phytoplankton in the upper ocean. *Limnol Oceanogr* 28:801–815.
13. Behrenfeld MJ, *et al.* (2006) Climate-driven trends in contemporary ocean productivity. *Nature* 444:752–755.
14. Dugdale RC, Wilkerson FP (1998) Silicate regulation of new production in the equatorial Pacific upwelling. *Nature* 391:270–273.
15. Tyrrell T (2008) Calcium carbonate cycling in future oceans and its influence on future climates. *J Plank Res* 30:141–156.
16. Brzezinski MA, Dumousseaud C, Krause JW, Measures CI, Nelson DM (2008) Iron and silicic acid concentrations together regulate Si uptake in the equatorial Pacific Ocean. *Limnol Oceanogr* 53:875–889.
17. Tilman D, Kilham SS, Kilham P (1982) Phytoplankton community ecology: The role of limiting nutrients. *Ann Rev Ecol Sys* 13:349–372.
18. Buithenius ET, Pangerc T, Franklin DJ, LeQuere C, Malin G (2008) Growth rates of six coccolithophorid strains as a function of temperature. *Limnol Oceanogr* 53:1181–1185.
19. Brown CW, Yoder JA (1994) Coccolithophorid blooms in the global ocean. *J Geophys Res* 99:7467–7482.
20. Denman K, Hofmann U, Marchant H (1996) *in Climate change 1995, The science of climate change*, eds Houghton JT, Meira Filho LG, Callander BA, Harris N, Kattenberg A, Maskell K (Cambridge Univ Press, Cambridge) pp. 483–516.
21. Bopp L, *et al.* (2001) Potential impact of climate change on marine export production. *Glob Biogeochem Cycles* 15:81–99.
22. Sarmiento JL, *et al.* (2004) Response of ocean ecosystems to climate warming. *Glob Biogeochem Cycles* 18:GB3003, doi:10.1029/2003GB002134.
23. Polovina JJ, Howell EA, Abecassis M (2008) Ocean's least productive waters are expanding. *Geophys Res Lett* 35:L03618, doi: 10.1029/2007GL031745.
24. Gregg WW, Conkright ME, Ginoux P, O'Reilly JE, Casey NW (2003) Ocean primary production and climate: Global decadal changes. *Geophys Res Lett* 30, 1809: doi: 10.1029/2003GL016889.
25. Dutkiewicz S, Sokolov A, Stone P, Scott J (2005) Joint Program of the Science and Policy of Global Change Report, 122 (Massachusetts Institute of Technology, Cambridge, MA).
26. Boyd PW, Doney SC (2002) Modelling regional responses by marine pelagic ecosystems to global climate change. *Geophys Res Lett* 29, 1806: doi: 10.1029/2001GL014130.
27. Bopp L, Amount O, Cadule P, Alvain S, Gehlen M (2005) Response of diatoms distribution to global warming and potential implications: A global model study. *Geophys Res Lett* 32:L19606.
28. Barber RT, Hiscock MR (2006) A rising tide lifts all phytoplankton: Growth response of other phytoplankton taxa in diatom-dominated blooms. *Glob Biogeochem Cycles* 20:GB4S03, doi:10.1029/2006GB002726.
29. Zondervan I, Zeebe RE, Rost B, Riebesell U (2001) Decreasing marine biogenic calcification: A negative feedback on rising atmospheric pCO$_2$. *Glob Biogeochem Cycles* 15:507–516.
30. Iglesias-Rodríguez MD, *et al.* (2008) Phytoplankton calcification in a high-CO$_2$ world. *Science* 320:336–340.
31. Riebesell U, *et al.* (2007) Enhanced biological carbon consumption in a high CO$_2$ ocean. *Nature* 450:545–548.
32. Falkowski PG, Oliver MJ (2007) Mix and match: How climate selects phytoplankton. *Nat Rev Microbiol* 5:813–819.
33. Antia A, *et al.* (2001) Basin-wide particulate carbon flux in the Atlantic Ocean: Regional export patterns and potential for atmospheric CO$_2$ sequestration. *Glob Biogeochem Cycles* 15:845–862.
34. Archer D, Winguth A, Lea D, Mahowald N (2000) What caused the glacial/interglacial pCO$_2$ cycles? *Revs Geophys* 38:159–189.
35. Holligan PM, *et al.* (1984) Vertical distribution and partitioning of organic carbon in mixed, frontal and stratified waters of the English Channel. *Mar Ecol Prog Ser* 14:111–127.
36. Sokolov A, Stone PH (1998) A flexible climate model for use in integrated assessments. *Climate Dynamics* 14:291–303.
37. Hansen J, *et al.* (1983) Efficient three-dimensional global models for climate studies: Models I and II. *Monthly Weather Review* 111:609–662.
38. Marshall JC, Hill C, Perelman L, Adcroft AJ (1997) Hydrostatic, quasi-hydrostatic, and nonhydrostatic ocean modelling. *J Geophys Res* 102:5733–5752.
39. Marshall JC, *et al.* (1997) A finite-volume, incompressible Navier Stokes model for studies of the ocean on parallel computers. *J Geophys Res* 102:5753–5766.
40. Gent P, McWilliams J (1990) Isopycnal mixing in ocean circulation models. *J Phys Oceanogr* 20:150–155.
41. Paltsev S, *et al.* (2005) Joint Program of the Science and Policy of Global Change Report 125 (MIT, Cambridge, MA).
42. Riebesell U, *et al.* (2000) Reduced calcification of marine plankton in response to increased atmospheric CO$_2$. *Nature* 407:364–367.
43. Sciandra A, *et al.* (2003) Response of coccolithophorid Emiliana huxleyi to elevated partial pressure of CO$_2$ under nitrogen limitation. *Mar Ecol Prog Ser* 261:111–122.
44. Feng Y, *et al.* (2008) Interactive effects of increased pCO2, temperature and irradiance on the marine coccolithophore *Emiliania huxleyi* (Prymnesiophyceae). *J Phycol* 43:87–89.
45. Burkhardt S, Zondervan I, Riebesell U (1999) Effect of CO2 concentration on C:NP ratio in marine phytoplankton: A species comparison. *Limnol Oceanogr* 44:683–690.

ECOLOGY